Indian Journal of Chemical Technology
Vol. 31, January 2024, pp. 26-30
DOI: 10.56042/ijct.v31i1.5500

Morphological studies of single phase alumina fabricated by wet milling method

Rupashree Dash[1,3]*, Laxmidhar Besra[2] & Sukalyan Dash[1]

[1]Department of Chemistry, Veer Surendra Sai University of Technology, Burla – 768 018, Odisha, India
[2]Department of Materials Chemistry, Institute of Minerals and Materials Technology (CSIR), Bhubaneswar – 751 013, Odisha, India
[3]Department of Science and Technology, Technology Bhavan, New Mehrauli Road, New Delhi – 110 016, India
*E-mail: rupashree.dash@gmail.com

Received 11 September 2023; accepted 12 December 2023

A wet milling process has been used as a novel method to fabricate single phase alumina. To fabricate the most thermodynamically stable form of alumina i.e., α-Al_2O_3, slurry method has been used here. α-Al_2O_3 has the widest band gap ~8.8 eV which makes it more valuable in electronic devices for use as a perfect insulator. Further, to confirm the surface morphology of the prepared α-Al_2O_3 sample, scanning electronic microscopy has been done. The prepared α-Al_2O_3 sample has been characterized using X-ray diffraction pattern, Fourier transform infra-red spectroscopy and photoluminescence spectroscopy. Raman spectroscopy of prepared α-Al_2O_3 has also been performed to understand the behaviour at microscopic level and also to confirm the purity of the single phase α-Al_2O_3 sample.

Keywords: Single phase alumina, α-Al_2O_3, Slurry, Wet milling

Introduction

Alumina (Al_2O_3) is one of the highly used refractory oxides[1-3] and is utilized in a wide range of applications, including high-strength materials, in electronics[4], ceramics, dielectric, optics[5,6], mechanical engineering, and catalysts[7-10]. It is considered as a perfect insulator for various applications like gate dielectric in metal-oxide-semiconductor field effect transistor[11-13] to trapping the insulator in charge blocking non-volatile memory cells, due to its wide bandgap, low leakage of current and high value of dielectric under ambient conditions. Al_2O_3 is known to exist in five metastable crystalline polymorphs[14-16] (transition aluminas), namely γ-Al_2O_3[17], η-Al_2O_3, δ-Al_2O_3, θ-Al_2O_3, and χ-Al_2O_3. In addition to these, α-Al_2O_3, also known as corundum or sapphire[18,19], is considered as one of the thermodynamically stable phases[20]. Among the various forms, two phases such as, α-Al_2O_3 and γ-Al_2O_3[21] are of great interest due to their technological applications. It is important to note that each form of Al_2O_3 is characterized by its own value of band gap[22, 23]. From the previously reported studies, the experimental value of band gap for γ-Al_2O_3 is 7.0-8.5 eV[24], for amorphous alumina i.e. am-Al_2O_3[25, 26], the band gap value is 5.0-7.0 eV and for α-Al_2O_3, the value of band gap[27] is higher, i.e. 8.8 eV, which makes it a perfect insulator. The band gap of Al_2O_3 depends upon the mode of its fabrication. Due to the high band gap of α-Al_2O_3 it becomes suitable for microelectronic devices, as a laser host material (e.g., Ruby laser), as a high strength window material, and as a dosimeter[28] using thermoluminescence readout[29]. During the last decade, α-Al_2O_3 or sapphire has been suggested as an efficient and reproducible dosimeter for both ultra-violet (UV) light and ionization radiation. It is thus important to work further on the structure[30] of α-Al_2O_3.

α-Al_2O_3 (0001) surface has p3 symmetry with Al atoms positioned at the centres of the 3-fold axis and oxygen positioned about the 3-fold axis in a hexagonal structure[31,32]. Unlike this, γ-Al_2O_3 has entirely different symmetry and has been described as a spinal similar to a traditional spinal AB_2O_4 structure. In γ-Al_2O_3, the oxygen atoms are arranged in a cubic close-packed lattice, while the A and B cations occupy the tetrahedral and octahedral interstitial sites of the lattice[33]. In order to fabricate pure α-Al_2O_3 with a high band gap, care must be taken of the surface and structural symmetry of the α-Al_2O_3 sample. Raman scattering is one of the most used non-destructive techniques to understand the microscopic properties and also is important to understand the behaviour of lattice vibrations in the molecule[34-37]. It is highly sensitive because of its ultra-sensitive probe which can quantify the smaller defect present in the sample[38-40]. Besides, advanced

technique such as the Raman spectro-microscopy adds to new capabilities of Raman spectroscopy[41,42] as a tool for understanding various aspects in different materials such as bulk materials, nanomaterials, thin films etc. This technique identifies various Raman active vibration modes[43], namely B_{1g}, E_g, and A_{1g} for various materials, which confirm the purity and phase of those materials. The other characterization[44] techniques such as X-ray diffraction (XRD), FTIR and PL spectroscopy are also used to determine the phase and surface structure and luminescent properties of the material.

The aim of the present work is to fabricate pure α-Al_2O_3 for various applications. Preparation has been carried out using wet milling slurry method, followed by characterization to confirm the formation of the sample. Room temperature XRD pattern and Raman spectra of the sample confirms the purity, FTIR analysis confirms the presence of required vibrational patterns and SEM reflects the surface morphology.

Experimental Section

Single phase α-Al_2O_3 has been fabricated by using slurry method, a two-step process. In the first step, slurry solution has been made in water medium using α-alumina (A-16SG) (ALCOA, USA) with average particle size of 300 nm. Darvan 821A of 40% aqueous solution of ammonium polyacrylate was used as the dispersant. The slurry was prepared in a polypropylene bottle containing two sizes of alumina balls of approximately 2 mm and 10 mm, respectively. The bigger balls fit the length of the bottle and smaller balls fit half of the slurry. Water, dispersant and N-(hydroxymethyl)acrylamide were taken within the polypropylene bottle to prepare 55% alumina powder slurry. To mix and wet the powder uniformly in the bottle, the powder was added in a step by step manner. Mixing of the solution was carried out in the planetary centrifugal mixer for several minutes for de-airing. Finally, ammonium persulfate (initiator) and tetramethylethylenediamine (catalyst) were added to the slurry with vigorous stirring and casted in the petroleum jelly coated Teflon mould at room temperature.

The second step involves drying and sintering process. The mould was covered with glass plate and kept in a preheated oven at 50°C for 2 h. Then cooling was done at 90% humid condition for 24 h to avoid cracking. The material was finally dried in an air-oven at 50°C for 24 h. Binder burnout was done by slow heating to completely remove the organics and after that sintering was done to produce the ceramic component.

Results and Discussion

The surface morphology and microstructure of the dried sample were studied using SEM. The SEM images (Fig. 1) show that a uniform crystalline structure has been formed. The top view of the SEM micrograph indicates that the α-Al_2O_3 sample contained a pure crystalline structure containing grey lines. A complete uniform structure can be seen from the Fig. 1a which has been recorded at low magnification ~10 μm. To understand and check the microstructure, SEM has also been recorded at high magnification ~1 μm (Fig. 1b) in which grey lines of the unit cells can be seen.

Further, phase purity and structural studies on the prepared α-Al_2O_3 sample have been carried out via XRD pattern, FTIR and Raman spectroscopy. The XRD pattern has been recorded at room temperature (300 K) from the diffraction angle (2θ values) 20º to 90º which can be seen in Fig. 2a.

The XRD pattern shows diffraction peaks at various 2θ values corresponding (h k l) planes, which can be identified as originating from the crystalline phase α-Al_2O_3. The corresponding miller indices (h k l) confirm the phase and plane present in the prepared sample. Al_2O_3 is known to have defects because of the

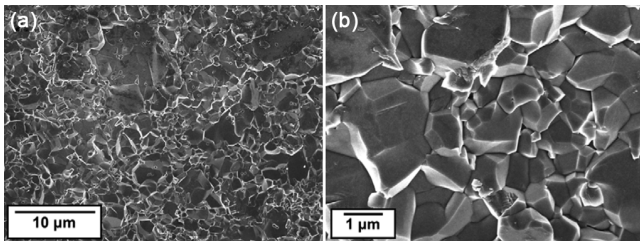

Fig. 1 — (a, b) SEM images of top surface morphology of α-Al_2O_3 at different magnifications

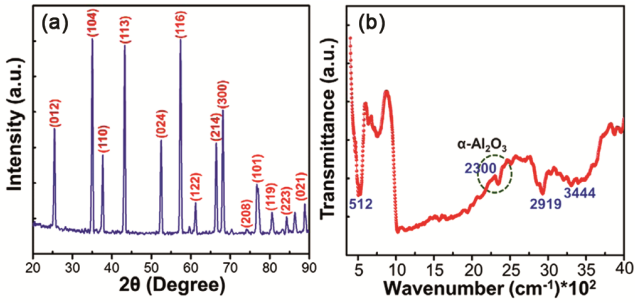

Fig. 2 — (a) X-Ray diffraction pattern and (b) FTIR spectrum of α-Al_2O_3 sample at room temperature

oxygen vacancy, where an O^{2-} ion moves from a normally occupied lattice site to a vacant interstitial site, which is supposed to be prevalent defect in many oxides. Under thermal conditions, hydrogen atom interacts with the lattice oxygen of Al_2O_3 on the surface, which results in the formation of the oxygen vacancies and changes the surface properties of α-Al_2O_3. No such defects could be identified through the XRD pattern. Furthermore, no additional peak or hump is seen in the XRD, which reveals that pure single phased α-Al_2O_3 have been fabricated.

The full width at half maximum (FWHM) values at each peak have been determined using ORIGIN software and corresponding crystallite sizes as well as its average value have been calculated using Debye-Scherrer formula (Eq. 1). The data matches the JCPDS-ICDD file number 46-1212. Average crystallite size was found to be 19.91 nm.

$$D = k/\beta Cos \quad ...(1)$$

where, D = crystallite size, K = Scherrer constant (0. 89), λ = wavelength (0.154 nm), β = FWHM.

FTIR spectrum (Fig. 2b) shows O-H stretching of α-Al_2O_3 sample at 3444 cm^{-1}. This stretching occurs only after 1230°C leading to the formation of the α-Al_2O_3 by the solid state thermally driven transformations from hydroxyl group of aluminium oxide. However, if the annealing temperature is below 1230°C, the possibility of dehydration level of this hydroxyl group is less, leading to the formation of γ-Al_2O_3. Hence, the degree of the transition to the α-Al_2O_3 or corundum structure depends on the time and the temperature of annealing treatment. Apart from this, the peak for alkyl halide was observed at 512 cm^{-1} upon verification with the present database and the spectrum matches with α-Al_2O_3. From Fig. 2b, it can be seen that a peak appearing at 2300 cm^{-1} corresponds to the α-Al_2O_3 phase, while for γ-Al_2O_3, a broad peak appears around 2300 cm^{-1} but with less value of transmittance. The FTIR data confirms the purity of the structure and chemical composition of the prepared α-Al_2O_3 sample.

The band gap energy of the sample has been calculated (Fig. 3a) from its absorption spectral studies (Fig. 3b). The λ_{max} value of the sample in aqueous medium is found to be 265 nm and the band gap energy has been calculated to be 5.47 eV.

To understand the molecular structure of the prepared α-Al_2O_3 crystalline sample, the bond structure diagram and the Raman spectrum have been

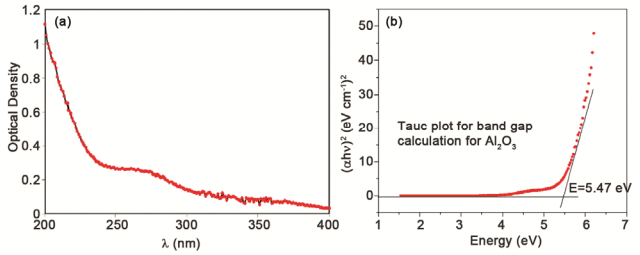

Fig. 3 — (a) Absorption spectrum with λ_{max} value of 265 nm and (b) Tauc plot for calculation of band gap of prepared alumina sample

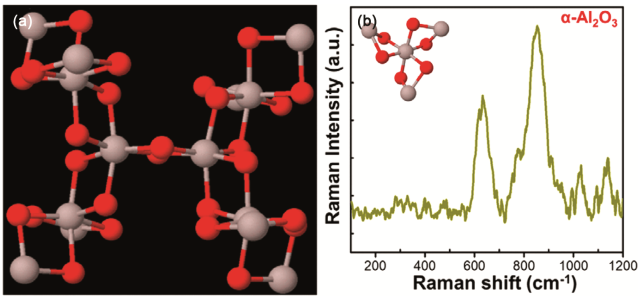

Fig. 4 — (a) Bond structure diagram of alumina using MolView software and (b) Raman spectrum of α-Al_2O_3 at 300K, inset shows the unit bond structure of alumina

presented. The molecular structure of α-Al_2O_3 sample has been generated (Fig. 4a) by using an online software, Mol View. The single phase structure shows the presence of two aluminium atoms attached with three oxygen atoms to complete the vacancies. Due to complexity of the structure, a singular structure of unit cell has been shown in the inset of the Fig. 4b. In the unit cell, grey and red sphere represent the aluminium and oxygen atoms, respectively. To deduce the structure at microscopic level, Raman spectrum of the compound (Fig. 4b) shows two broad Raman active modes at 650 cm^{-1} and 875 cm^{-1}. It is well known that in case of γ-Al_2O_3, Raman mode appears at 630 cm^{-1} and 700 cm^{-1}. However, γ-Al_2O_3 also shows an additional peak compared to α-Al_2O_3. There are two more Raman active modes present in the α-Al_2O_3 Raman spectrum at 380 cm^{-1} and 420 cm^{-1} but these modes are very low intense as compare to the other ones (above mentioned), which can be seen in the spectrum. The structural and spectroscopic analysis confirm that the prepared sample of Al_2O_3 is in single phase and has the α-form, which is thermodynamically the most stable phase.

Conclusion

In summary, pure crystalline α-Al_2O_3 has been prepared by wet milling method (slurry method) and

confirmation to this effect is obtained from various well documented characterization techniques. Scanning electron microscopy at different magnifications has been performed to see the top surface morphology of the prepared α-Al_2O_3 sample, which confirms the uniformity of the single phase of α-Al_2O_3 sample. Raman spectroscopy of the material shows two Raman active modes confirming the presence of α-Al_2O_3. A fair agreement in all the spectral data has been reached.

Acknowledgement

The authors are thankful for the facilities by Nano Science and Technology Center, Jamia Millia Islamia, New Delhi, Department of Materials Chemistry, CSIR-Institute of Minerals and Materials Technology, Bhubaneswar and Department of Physics, IIT Indore for characterization of the materials.

References

1 Ghanbari A K, Sharp J H & Lee W E, Hydration of refractory oxides in castable bond systems-I: Alumina, magnesia, and alumina-magnesia mixtures, *J Eur Ceram Soc*, 22 (2002) 495.

2 Emblem H G & Davies T J, Solid-state chemistry of alumina-chrome refractories, *Rev Inorg Chem*, 13 (1993) 103.

3 Peng N, Deng C, Zhu H, Li J & Wang S, Effects of alumina sources on the microstructure and properties of nitrided Al_2O_3-C refractories, *Ceram Int*, 41 (2015) 5513.

4 Nasiri A & Ang S, Application of Alumina-based ceramic paste for high-temperature electronics packaging, *J Electron Packag*, 143 (2021) 020902.

5 Chen J, Wheeler V M, Liu B Kumar A Coventry J & Lipiński W, Optical characterisation of alumina-mullite materials for solar particle receiver applications, *Sol Energy Mater Sol Cells*, 230 (2021) 111170.

6 Kumeria T, Santos A & Losic D, Nanoporous anodic alumina platforms: engineered surface chemistry and structure for optical sensing applications, *Sensors*, 14 (2014) 11878.

7 Meyza X, Goeuriot D, Guerret-Piécourt C, Tréheux D & Fitting H J, Secondary electron emission and self-consistent charge transport and storage in bulk insulators: Application to alumina, *J Appl Phys*, 94 (2003) 5384.

8 Evans A G, A method for evaluating the time-dependent failure characteristics of brittle materials and its application to polycrystalline alumina, *J Mater Sci*, 7 (1972) 1137.

9 Hirashima H, Kojima C & Imai H, Application of alumina aerogels as catalysts, *J Sol Gel Sci Technol*, 8 (1997) 843.

10 Rajiv G M, Viswanathan N & Meenakshi S, Preparation and application of alumina/chitosan biocomposite**,** *Int J Biol Macromol*, 47 (2010) 146.

11 Oshima K, Cristoloveanu S, Guillaumot B, Iwai H & Deleonibus S, Advanced SOI MOSFETs with buried alumina and ground plane: self-heating and short-channel effects, *Solid State Electron*, 48 (2004) 907.

12 Gutiérrez M, Lloret F, Pham T T, Cañas J, Reyes D F, Eon D, Pernot J & Araújo D, Control of the alumina microstructure to reduce gate leaks in diamond MOSFETs, *Nanomaterials*, 8 (2018) 584.

13 Uchida N, Nakajima Y, Bolotov L, Chang W H, Maeda T & Ohishi Y, Heat transport properties of alumina Gate insulator films on Ge substrates fabricated by atomic layer deposition, *Mater Sci Semicond Process*, 121 (2021) 105396.

14 Kovarik L, Bowden M & Szanyi J, High temperature transition aluminas in δ-Al_2O_3/θ-Al_2O_3 stability range: Review, *Rev J Catal*, 393 (2021) 357.

15 Kovarik L, Bowden M, Shi D, Washton N M, Andersen A, Hu J Z, Lee J, Szanyi J, Kwak J H & Peden C H F, Unraveling the origin of structural disorder in high temperature transition Al_2O_3: Structure of θ-Al_2O_3, *Chem Mater*, 27 (2015) 7042.

16 Amrute A P, Jeske K, Łodziana Z, Prieto G & Schüth F, Hydrothermal stability of high-surface-area α-Al_2O_3 and its use as a support for hydrothermally stable Fischer–Tropsch synthesis catalysts, *Chem Mater*, 32 (2020) 4369.

17 Rotole J A & Sherwood P M A, Gamma-alumina (γ-Al_2O_3) by XPS, *Surf Sci Spectra*, 5 (1998) 18.

18 Dynys F W & Halloran J W, Alpha alumina formation in alum-derived gamma alumina, *J Am Ceram Soc*, 65 (1982) 442.

19 Cahoon H P & Christensen C J, Sintering and grain growth of alpha-alumina, *J Am Ceram Soc*, 39 (1956) 337.

20 Rossignol S & Kappenstein C, Effect of doping elements on the thermal stability of transition alumina, *Int J Inorg Mater*, 3 (2001) 51.

21 Castro R H R, Ushakov S V, Gengembre L, Gouvêa D & Navrotsky A, Surface energy and thermodynamic stability of γ-alumina: Effect of dopants and water, *Chem Mater*, 18 (2006) 1867.

22 Yan P, Tao F G, Liang S G, Wu B & Zhang L D, Fabrication of one-dimensional alumina photonic crystals with a narrow band gap and their application to high-sensitivity sensors, *J Mater Chem C*, 1 (2013) 1659.

23 Costina I & Franchy R, Band gap of amorphous and well-ordered Al_2O_3 on Ni_3Al(100), *Appl Phys Lett*, 78 (2001) 4139.

24 Filatova E O & Konashuk A S, Interpretation of the changing the band gap of Al_2O_3 depending on its crystalline form: connection with different local symmetries, *J Phys Chem C*, 119 (2015) 20755.

25 Momida H, Hamada T, Takagi Y, Yamamoto T, Uda T & Ohno T, Theoretical study on dielectric response of amorphous alumina, *Phys Rev B*, 73 (2006) 054108.

26 Mavrič A, Valant M, Cui C & Wang Z M, Advanced applications of amorphous alumina: From nano to bulk, *J Non Cryst Solids*, 521 (2019) 119493.

27 Santos R C R, Longhinotti E, Freire V N, Reimberg R B & Caetano E W S, Elucidating the High-k Insulator α-Al_2O_3 direct/indirect energy band gap type through density functional theory computations, *Chem Phys Lett*, 637 (2015) 172.

28 Ekendahl D & Judas L, Retrospective dosimetry with alumina substrate from electronic components, *Radiat Protect Dosim*, 150 (2012) 134.

29 Summers G P, Thermoluminescence in single crystal alpha-Al_2O_3, *Radiat Prot Dosim*, *8* (1984) 69.

30 Ciraci S & Batra I P, Electronic structure of α-alumina and Its defect states, *Phys Rev B*, 28 (1983) 982.
31 Perevalov T V, Shaposhnikov A V, Gritsenko V A, Wong H, Han J H & Kim C W, Electronic Structure of α-Al2O3: Ab Initio Simulations and Comparison with Experiment, *JETP Lett*, 85 (2007) 165.
32 Rahane A B, Deshpande M D & Kumar V, Structural and electronic properties of $(Al_2O_3)_n$ clusters with n = 1–10 from first principles calculations, *J Phys Chem C*, 115 (2011) 18111.
33 Liu Y, Cheng B, Wang K K, Ling G P, Cai J, Song C L & Han G R, Study of Raman spectra for γ-Al_2O_3 models by using first-principles method, *Solid State Commun*, 178 (2014) 16.
34 Raman C V & Krishnan K S, New type of secondary radiation, *Nature*, 121 (1928) 501.
35 Raman C V, A new radiation, *Proc Indian Acad Sci*, 37 (1953) 333.
36 Beeman D, Tsu R & Thorpe M F, Structural information from the Raman spectrum of amorphous silicon, *Phys Rev B*, 32 (1985) 874.
37 Balkanski M, Wallis R F & Haro E, Anharmonic effects in light scattering due to optical phonons in silicon, *Phys Rev B*, 28 (1983) 1928.
38 Rani C, Pathak D K, Tanwar M, Kandpal S, Ghosh T, Yu M M & Kumar R, Anharmonicity induced faster decay of hot phonons in rutile TiO_2 nanorods: A Raman spectromicroscopy study, *Mater Adv*, 3 (2022) 1602.
39 Rani C, Tanwar M, Ghosh T, Kandpal S, Pathak D K, Chaudhary A, Yogi P, Saxena S K & Kumar R, Raman spectroscopy as a simple yet effective analytical tool for determining Fermi energy and temperature dependent Fermi shift in silicon, *Anal Chem*, 94 (2022) 1510.
40 Rani C, Tanwar M, Kandpal S, Ghosh T, Bansal L & Kumar R, Nonlinear temperature-dependent phonon decay in heavily doped silicon: Predominant interferon-mediated cold phonon annihilation, *J Phys Chem Lett*, 13 (2022) 5232.
41 Rani C, Tanwar M, Kandpal S, Ghosh T, Pathak D K, Chaudhary A & Kumar R, Predicting Raman line shapes from amorphous silicon clusters for estimating short-range Order, *J Raman Spectrosc*, 52 (2021) 2081.
42 Ferraro J R, Introductory Raman Spectroscopy; *Elsevier*, (2003).
43 Cerdeira F, Fjeldly T A & Cardona M, Effect of free carriers on zone-center vibrational modes in heavily doped *p*-type Si. II. Optical modes, *Phys Rev B*, 8 (1973) 4734.
44 Parida K M, Pradhan A C, Das J & Sahu N, Synthesis and characterization of nano-sized porous gamma-alumina by control precipitation method, *Mater Chem Phy*, 113 (2009) 244.